

Accepted Manuscript

Research paper

Dipalladium(I) complexes of *ortho*- and *para*-functionalized 1,3-Bis(aryl)triazenide ligands: synthesis, structure and catalytic activity

Erick Correa-Ayala, Carlos Campos-Alvarado, Daniel Chávez, Simón Hernández-Ortega, David Morales-Morales, Valentín Miranda-Soto, Miguel Parra-Hake

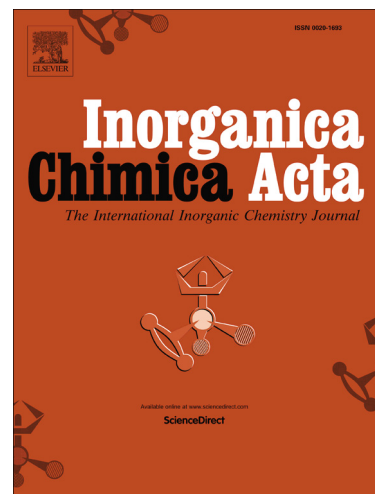
PII: S0020-1693(18)31844-9
DOI: <https://doi.org/10.1016/j.ica.2019.03.004>
Reference: ICA 18809

To appear in: *Inorganica Chimica Acta*

Received Date: 18 December 2018
Revised Date: 1 March 2019
Accepted Date: 4 March 2019

Please cite this article as: E. Correa-Ayala, C. Campos-Alvarado, D. Chávez, S. Hernández-Ortega, D. Morales-Morales, V. Miranda-Soto, M. Parra-Hake, Dipalladium(I) complexes of *ortho*- and *para*-functionalized 1,3-Bis(aryl)triazenide ligands: synthesis, structure and catalytic activity, *Inorganica Chimica Acta* (2019), doi: <https://doi.org/10.1016/j.ica.2019.03.004>

This is a PDF file of an unedited manuscript that has been accepted for publication. As a service to our customers we are providing this early version of the manuscript. The manuscript will undergo copyediting, typesetting, and review of the resulting proof before it is published in its final form. Please note that during the production process errors may be discovered which could affect the content, and all legal disclaimers that apply to the journal pertain.



Dipalladium(I) complexes of *ortho*- and *para*-functionalized 1,3-Bis(aryl)triazenide ligands: synthesis, structure and catalytic activity

Erick Correa-Ayala^a, Carlos Campos-Alvarado^a, Daniel Chávez^a, Simón Hernández-Ortega^b,
David Morales-Morales^b, Valentín Miranda-Soto^{a,*}, Miguel Parra-Hake^{a,*}

^a*Tecnológico Nacional de México/Instituto Tecnológico de Tijuana, Centro de Graduados e Investigación en Química, Apartado Postal 1166, Tijuana, B.C. 22000, México*

^b*Instituto de Química, Universidad Nacional Autónoma de México, Circuito Exterior. Cd. Universitaria Coyoacán, México D.F. 04510, México*

Abstract

The synthesis and characterization of a series dipalladium(I) complexes of formulae [Pd{1-[2'-(methoxycarbonyl)phenyl]-3-[4'-X-phenyl]triazenide}]₂ [X = F (**4**), Cl (**5**), Br (**6**)] are reported. The crystal structure of complex **4** was determined by X-ray diffraction studies. The previously reported dipalladium(I) **1** to **3** as well as the new complexes **4** to **6** were used as catalysts in the Heck and Suzuki couplings of different *p*-substituted bromobenzenes.

Keywords: Triazenide ligands, Pd(I) complexes, Catalysis, Cross coupling reactions, Heck couplings, Suzuki-Miyaura couplings.

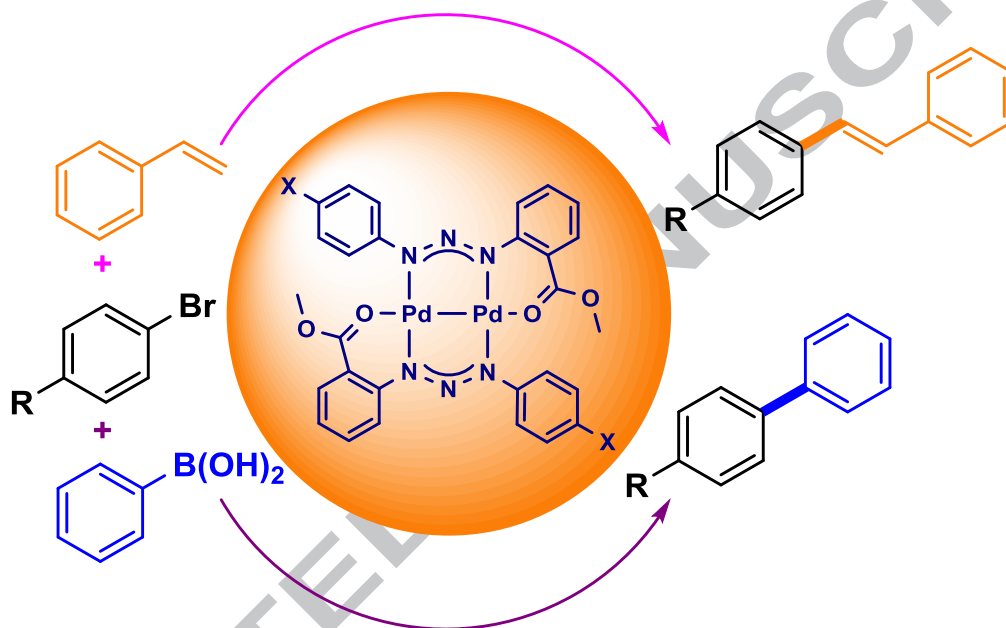
Highlights

- Triazenide Pd(I) dinuclear complexes were obtained
- The Pd(I) dinuclear complexes are efficient catalysts in Heck and Suzuki couplings
- Substituents in the triazenide ligands are relevant in their catalytic activity

ACCEPTED MANUSCRIPT

Graphical abstract

The series of dipalladium(I) complexes [Pd{1-[2'-(methoxycarbonyl)phenyl]-3-[4'-X-phenyl]triazenide}]₂ [X = F (**4**), Cl (**5**), Br (**6**)] were synthesized and used as efficient catalysts in Heck and Suzuki-Miyaura couplings of different *p*-substituted bromobenzenes.



1. Introduction

Catalysis using dinuclear transition metal complexes has recently received considerable attention [1-5] since cooperation of two metal centers can improve the selectivity and efficiency of the catalyst and promote reactions that are not possible using a single metal center. In this context, dinuclear complexes with the relatively rare Pd^I oxidation state have emerged as a promising class of catalysts for cross-coupling reactions [6-24].

The challenge in designing dipalladium(I) catalysts lays in the selection of ligands capable of stabilizing the Pd^I and to adequately respond to geometric and electronic reorganization of the bimetallic core during the course of the catalytic cycle. 1,3-bis(aryl)triazenides are a promising choice due to their propensity to coordinate in a bridging fashion stabilizing bimetallic cores in a variety of oxidation states [25-29]. The traditional 1,3-bis(aryl)triazenide ligands stabilize the common Pd^{II} oxidation state [30-33] but are not capable of stabilizing the Pd^I-Pd^I core. However, our research group has reported the first dipalladium(I)-triazenide complexes by using *ortho*-functionalized 1,3-bis(aryl)triazenide ligands (Figure 1) [34]. It was found that the Pd^I-Pd^I core was stabilized when hard weakly coordinating groups in the triazenide ligand were used (**1-3**). This and other reports of our research group have shown that the *ortho*-substituents in the 1,3-bis(aryl)triazenide ligands can have a dramatic impact on the chemistry [35-37] and catalytic activity [38-40] of their complexes.

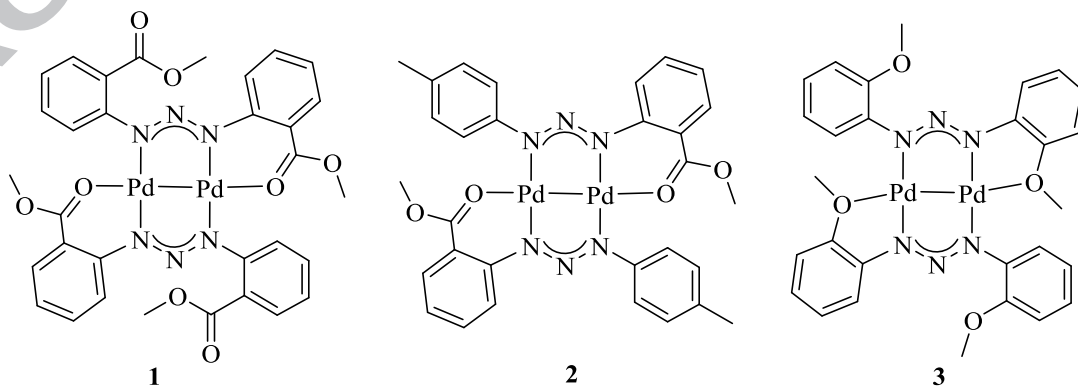


Figure 1. Dipalladium-triazenide complexes (**1-3**) previously reported [34].

More recently, a couple of dipalladium(I) complexes supported by *ortho*-functionalized 1,3-bis(aryl)triazenide ligands have been reported by Zhan and co-workers [41,42]. Furthermore, Úbeda and co-workers reported the synthesis, characterization and DFT calculations of some dipalladium(I)-triazenide complexes, including the previously reported complex **3** [43]. However, noteworthy the fact that there are not previous reports of dipalladium(I)-triazenide complexes used as catalyst in cross-coupling reactions.

Thus, we report here the synthesis and characterization of three new dipalladium(I)-triazenide complexes of formula $[\text{Pd}\{1\text{-}[2'\text{-(methoxycarbonyl)phenyl]}\text{-}3\text{-}[4'\text{-X-phenyl]triazenide}\}]_2$ [X = F (**4**), Cl (**5**), Br (**6**)]. The objective is to determine the catalytic activity of these three new complexes and the previously reported dipalladium(I) complexes **1-3** [34] in C-C cross-coupling reactions. It was expected that the relative catalytic efficiency to be dependent on the *ortho*-substituent in complexes **1-3** and the *para*-substituent in complexes **4-6**.

2. Experimental Section

2.1. General comments

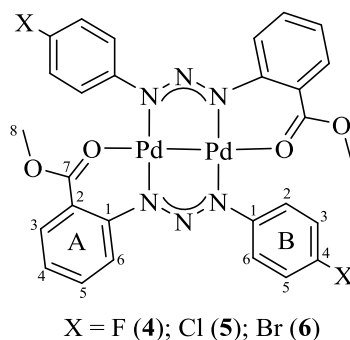
All synthetic work was carried out in air or under argon using standard Schlenk techniques or an inert atmosphere dry-box, where indicated. All solvents were dried over appropriate drying agents. PdCl₂ (Aldrich) and other reagents are commercially available and were used as received. $[\text{Pd}(\text{CH}_3\text{CN})_2(\text{Cl})_2]$ [44], 1-[2'-(methoxycarbonyl)phenyl]-3-[4'-(fluoro)phenyl]triazene (**L1**) [40], 1-[2'-(methoxycarbonyl)phenyl]-3-[4'-(chloro)phenyl]triazene (**L2**) [40], 1-[2'-(methoxycarbonyl)phenyl]-3-[4'-(bromo)phenyl]triazene (**L3**) [40], $[\text{Pd}\{1,3\text{-bis}[2'\text{-(methoxycarbonyl)phenyl]triazenide}\}]_2$ (**1**) [34], $[\text{Pd}\{1\text{-}[2'\text{-(methoxycarbonyl)phenyl]}\text{-}3\text{-}[4'\text{-methylphenyl]triazenide}\}]_2$ (**2**) [34] and $[\text{Pd}\{1,3\text{-bis}[2'\text{-(methoxy)phenyl]triazenide}\}]_2$ (**3**) [34] were synthesized according to previously reported procedures. NMR spectra were recorded at 400 MHz with a Bruker Avance III spectrometer at 30 °C unless otherwise specified. ¹H and ¹³C NMR chemical shifts are reported in ppm referenced to residual solvent resonances (¹H NMR: 7.16 for C₆HD₅ in C₆D₆, 1.94 for CHD₂CN in CD₃CN, 2.05 for acetone-*d*₅ in acetone-*d*₆. ¹³C NMR: 128.39, 1.39, and 29.92 for benzene-*d*₆, acetonitrile-*d*₃ and acetone-*d*₆, respectively). Coupling constants *J* are given in Hertz (Hz). IR spectra were recorded on a Perkin-Elmer FT-

IR 1605 spectrophotometer. Melting points were measured in an Electrothermal GAC 88629 apparatus. Mass spectra were obtained by direct insertion on an Agilent Technologies 59756 Instrument. High Resolution Mass Spectrometry (HRMS) data were obtained in a micrOTOF-Q III MS instrument with electrospray ionization using sodium formate as calibrant.

2.2. Synthesis of complexes

2.2.1. [Pd{1-[2'-(methoxycarbonyl)phenyl]-3-[4'-fluorophenyl]triazenide}]₂ (**4**)

Triazene **L1** (52.65 mg, 0.1927 mmol, 1.0 eq) was dissolved in CH₃CN (5 mL), to this solution triethylamine (38.94 mg, 0.3854 mmol, 2 eq) was added with stirring. To the resulting reaction mixture, a solution of [Pd(CH₃CN)₂(Cl)₂] (50 mg, 0.1927 mmol, 1.0 eq) in CH₃CN (5 mL) was slowly added, and the resulting mixture was stirred for 30 min at room temperature, during which time a red precipitate formed. The reaction mixture was filtered to obtain a reddish microcrystalline solid, which was recrystallized by vapor diffusion of pentane into a concentrated solution of the product in CH₂Cl₂ at room temperature to give red crystals, suitable for X-ray diffraction analysis (53.17 mg, 0.0703 mmol, 73%). MP = 198–201 °C. IR(KBr): 3014, 2957, 1652, 1595, 1557, 1499, 1428, 1368, 1251, 1187, 1084, 826, 748 cm⁻¹. ¹H NMR [CDCl₃, 400 MHz]: δ 7.85 (dd, *J* = 8.4, 1.6 Hz, 2H, Ar_{A3}), 7.54 (dd, *J* = 8.4, 1.2 Hz, 2H, Ar_{A6}), 7.37 (dd, *J* = 9.2, 5.2 Hz, 4H, Ar_{B2,6}), 7.33 (td, *J* = 7.2, 1.6 Hz, 2H, Ar_{A5}), 6.98 (t, *J* = 8.8 Hz, 4H, Ar_{B3,5}), 6.93 (td, *J* = 8.4, 1.2 Hz, 2H, Ar_{A4}), 3.62 (s, 6H, OCH_{3(A7)}). ¹³C {¹H} NMR [CDCl₃, 100 MHz]: δ 169.8 (C_{A7}), 161.1 (d, *J* = 243.0 Hz, C_{B4}), 151.8 (C_{A1}), 146.9 (d, *J* = 2.0 Hz, C_{B1}), 134.3 (C_{A5}), 131.9 (C_{A3}), 124.7 (d, *J* = 8.0 Hz, C_{B2,6}), 122.2 (C_{A4}), 120.0 (C_{A6}), 116.9 (C_{A2}), 114.7 (d, *J* = 22.0 Hz, C_{B3,5}), 53.8 (C_{A8}). HRMS (ESI-TOF) *m/z*: [M + Na] Calc. for C₂₈H₂₂N₆O₄F₂Pd₂Na 780.9649; Found 780.9647. Anal. Calc. for C₂₈H₂₂N₆O₄F₂Pd₂ (757.36): C, 44.40; H, 2.93; N, 11.10. Found, C, 44.19; H, 2.85; N, 11.04.



2.2.2. [Pd{1-[2'-(methoxycarbonyl)phenyl]-3-[4'-chlorophenyl]triazene}]₂ (**5**)

Complex **5** was prepared in the same manner as **4** using triazene **L2** (55.82 mg, 0.1927 mmol, 1.0 eq). Red crystals (49.34 mg, 0.0626 mmol, 65%). MP = 222–224 °C. IR(KBr): 3023, 2937, 1651, 1557, 1476, 1433, 1358, 1194, 1157, 1085, 819, 752 cm⁻¹. ¹H NMR [CDCl₃, 400 MHz]: δ 7.86 (dd, *J* = 8.4, 1.6 Hz, 2H, Ar_{A3}), 7.53 (dd, *J* = 8.4, 0.8 Hz, 2H, Ar_{A6}), 7.37 (d, *J* = 8.8 Hz, 4H, Ar_{B2,6}), 7.35 (td, *J* = 8.4, 1.6 Hz, 2H, Ar_{A5}), 7.23 (d, *J* = 8.8 Hz, 4H, Ar_{B3,5}), 6.97 (td, *J* = 8.0, 1.2 Hz, 2H, Ar_{A4}), 3.66 (s, 6H, OCH_{3(A8)}). ¹³C {¹H} NMR [CDCl₃, 100 MHz]: δ 169.8 (C_{A7}), 151.6 (C_{A1}), 149.3 (C_{B1}), 134.3 (C_{A5}), 131.9 (C_{A3}), 131.1 (C_{B4}), 128.1 (C_{B3,5}), 124.4 (C_{B2,6}), 122.5 (C_{A4}), 120.2 (C_{A6}), 117.2 (C_{A2}), 53.9 (C_{A8}). HRMS (ESI-TOF) *m/z*: [M + Na] Calc. for C₂₈H₂₂N₆O₄Cl₂Pd₂Na 812.9046; Found 812.9042. Anal. Calc. for C₂₈H₂₂N₆O₄Cl₂Pd₂ (790.26): C, 42.56; H, 2.81; N, 10.63. Found, C, 42.58; H, 2.78; N, 10.52.

2.2.3. [Pd{1-[2'-(methoxycarbonyl)phenyl]-3-[4'-bromophenyl]triazene}]₂ (**6**)

Complex **6** was prepared in the same manner as **4** using triazene **L3** (64.39 mg, 0.1927 mmol, 1.0 eq). Red crystals (38.87 mg, 0.0443 mmol, 46%). MP = 234–236 °C. IR(KBr): 3023, 2937, 1650, 1560, 1476, 1355, 1193, 1157, 1080, 818, 753 cm⁻¹. ¹H NMR [CDCl₃, 400 MHz]: δ 7.86 (dd, *J* = 8.4, 1.6 Hz, 2H, Ar_{A3}), 7.53 (dd, *J* = 8.4, 0.8 Hz, 2H, Ar_{A6}), 7.38 (d, *J* = 8.8 Hz, 4H, Ar_{B3,5}), 7.35 (m, 2H, Ar_{A5}), 7.32 (d, *J* = 8.8 Hz, 4H, Ar_{B2,6}), 6.97 (td, *J* = 8.4, 1.2 Hz, 2H, Ar_{A4}), 3.66 (s, 6H, OCH_{3(A8)}). ¹³C {¹H} NMR [CDCl₃, 100 MHz]: δ 169.8 (C_{A7}), 151.6 (C_{A1}), 149.7 (C_{B1}), 134.3 (C_{A5}), 131.9 (C_{A3}), 131.1 (C_{B3,5}), 124.8 (C_{B2,6}), 122.6 (C_{A4}), 120.2 (C_{A6}), 119.0 (C_{B4}), 117.2 (C_{A2}), 53.9 (C_{A8}). HRMS (ESI-TOF) *m/z*: [M + Na] Calc. for

C₂₈H₂₂N₆O₄Br₂Pd₂Na 902.8026; Found 902.8023. Anal. Calc. for C₂₈H₂₂N₆O₄Br₂Pd₂ (879.17): C, 38.25; H, 2.52; N, 9.56; Found, C, 38.10; H, 2.47; N, 9.49.

2.3. X-ray crystallography

A yellow prism crystal of compound **4**, was grown from CH₂Cl₂/diethyl ether and mounted on a glass fiber, then placed on a Bruker Smart Apex II diffractometer with a Mo-target X-ray source ($\lambda = 0.71073\text{\AA}$). The detector was placed at a distance of 5.0 cm from the crystal and frames were collected with a scan width of 0.5 in ω and exposure time of 10 s/frame. 9883 reflections were collected and integrated with the Bruker SAINT software package using a narrow-frame integration algorithm. Systematic absences and intensity statistics were used in monoclinic P2/c space group. The structure was solved using Patterson methods using SHELXS-2014/7 program [45]. The remaining atoms were located via a few cycles of least squares refinements and difference Fourier maps. Hydrogen atoms were input at calculated positions and allowed to ride on the atoms to which they are attached. Thermal parameters were refined for hydrogen atoms on the phenyl groups using a Ueq = 1.2 \AA^2 and 1.5 for methyl groups. The final cycle of refinement was carried out on all non-zero data using SHELXL-2014/7 [45]. Absorption correction was applied using SADABS program. The structure was solved as a half of molecule, and symmetry plane is needed to generate the whole molecule. Crystallographic data and refinement parameters are shown in Table S1.

2.4. General procedure for Heck couplings

In open air, a Schlenk tube equipped with a magnetic stirring bar was charged with DMF (3 mL), aryl halide (6.369 mmol), alkene (6.369 mmol), 1.2 eq of base and the catalyst (3.582×10^{-3} mmol). The tube was sealed and fully immersed in a 120 °C silicon oil bath. After the prescribed reaction time, the mixture was cooled to room temperature and the organic phase was analyzed by gas chromatography-mass spectrometry (GC-MS).

2.5. General procedure for Suzuki couplings

In open air, a Schlenk tube equipped with a magnetic stirring bar was charged with DMF (3 mL), aryl halide (6.369 mmol), boronic acid (6.369 mmol), 1.2 eq of base and the

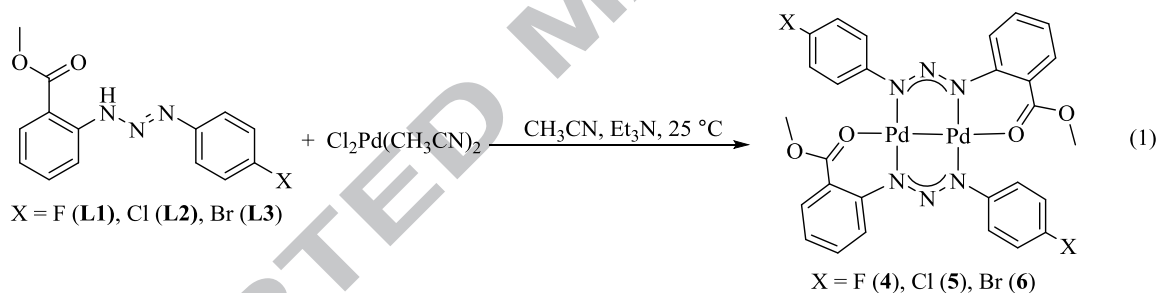
catalyst (3.582×10^{-3} mmol). The tube was sealed and fully immersed in a 100 °C silicon oil bath. After the prescribed reaction time, the mixture was cooled to room temperature and the organic phase was analyzed by gas chromatography-mass spectrometry (GC-MS).

3. Results and discussion

3.1. Synthesis and general characterization

3.1.1. Dipalladium(I) complexes

The synthesis and characterization of triazenes **L1-L3** [40] and complexes **1-3** [34] have been described previously. Complexes **4-6** were prepared by combination of bis(acetonitrile)-palladium(II) dichloride in acetonitrile with a mixture of the corresponding triazene (**L1-L3**) and triethylamine at room temperature (Eq. 1). The air- and moisture-stable red complexes were purified after recrystallization (dichloromethane/pentane) with yields in the range of 73-46%.



As is the case for complexes **1-3** (Figure 1) analytical and spectroscopic data (IR, NMR and HRMS), and X-ray crystal structure determination revealed dipalladium(I) complexes (Eq. 1). It is assumed that the d^9 Pd(I) centers are spin coupled through a Pd-Pd bond, since the d^9 configuration is expected to exhibit paramagnetic behavior and compounds **4-6** are diamagnetic and amenable to NMR analysis. This behavior has been previously observed in other dipalladium(I) complexes [46-54]. Reduction of Pd(II) to Pd(I) is attributed to the triethylamine used for the deprotonation of the triazene to form the triazene ligand, as reported by Walsh for the synthesis of complexes **1-3** [34]. Similarly, Lu and Peters found that a related bis(phosphine)Pd(II) complex was reduced to Pd(I) in good yield in the presence of an excess of a tertiary amine [55].

The ^1H and ^{13}C $\{^1\text{H}\}$ NMR data of complexes **4-6** are summarized in Tables S3 and S4, respectively. The integration of sixteen hydrogens in the aromatic region (7.86–6.93 ppm) of each complex corresponds to the presence of two equivalent triazenide ligands. The methoxy group appears as a singlet at ~ 3.64 ppm and integrates for six hydrogens. The ^{13}C $\{^1\text{H}\}$ NMR spectra of complexes **4-6** show a single carbonyl signal at 169.8 ppm, slightly downfield from the unbound ligands (167.7 ppm) [40]. The spectra of complexes **5** and **6** showed 10 signals for the carbon atoms in the aromatic region, while that of complex **4**, exhibits the carbons in the aromatic ring B as doublets, due to the coupling with the *p*-F (Table S4). Interestingly, as a result of the σ -acceptor and π -donor effects of the *para*-halogen substituents [56], for complexes **4** (*p*-F, 161.1 ppm), **5** (*p*-Cl, 131.1 ppm) and **6** (*p*-Br, 119.0 ppm), the signals due to the B4 carbons are shifted downfield, as the *para*-halogen substituent becomes more electronegative.

3.2. Description of the crystal structure

X-ray quality crystals were obtained from vapor phase diffusion of pentane into a concentrated solution of complex **4** in dichloromethane. The ORTEP diagram of **4** is shown in Figure 2.

The molecular structure of **4** consists of two directly bonded palladium(I) atoms bridged by two mutually *trans* triazenide ligands. The structure has a C2 symmetry axis rendering the atoms equivalent by symmetry. The oxygen atom of the *o*-methoxycarbonyl substituent occupies the site *trans* to the Pd₁-Pd₁ axis.

The structure shows a slightly distorted square planar geometry with N₃-Pd₁-O₁, O₁-Pd₁-N₁, N₁-Pd₁-Pd₁ and N₃-Pd₁-Pd₁ angles of 86.58(15), 101.66(15), 84.27(11) and 87.47(11)°, respectively. The Pd-N distances (ca. 2.02 Å), the N-N bonds nearly equivalent (~ 1.31 Å) and the N₁-N₂-N₃ angle of 115.30(4)° indicate a pronounced π delocalization around the metal-triazenide system.

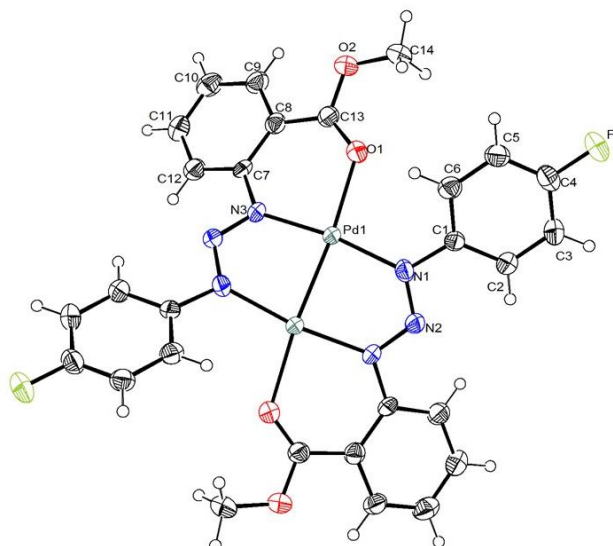


Figure 2. Molecular structure of **4** (H atoms are omitted for clarity; thermal ellipsoid set at 30% probability). Bond lengths (Å): Pd₁-Pd₁, 2.3999(8); Pd₁-N₁, 2.031(4); Pd₁-N₃, 2.016(4); Pd₁-O₁, 2.198(4); N₁-N₂, 1.311(6); N₂-N₃, 1.315(6); C₄-F₁, 1.369(6); C₁₃-O₁, 1.219(6). Bond angles (°): N₁-N₂-N₃, 115.30(4); Pd₁-Pd₁-O₁, 174.00(10); Pd₁-Pd₁-N₁, 84.27(11); Pd₁-Pd₁-N₃, 87.47(11); N₁-Pd₁-N₃, 171.69(16); N₁-Pd₁-O₁, 101.66(15); N₃-Pd₁-O₁, 86.58(15); O₁-C₁₃-O₂, 119.70(5).

Although the structural values are consistent with the closely related complexes **1** and **2** [34] (Figure 1), there are some important differences. For instance, complexes **4** (*p*-fluorophenyl, 15.52°) and **2** (*p*-tolyl, 53.81°) differ in the dihedral angle (Φ) formed between the NNN plane. The smaller dihedral angle in **4** suggests a stronger π delocalization of the triazenide system into the *p*-fluorophenyl ring as a result of the electronic effect induced by the *p*-F [57].

Also, in contrast to the structure of complexes **1-3**, and other related dipalladium(I)-triazenide complexes [41-43], in complex **4** the eight-membered Pd₂(NNN)₂ ring, is not planar. The molecule adopts a "twist boat configuration", with a torsion angle N₁-Pd₁-Pd₁-N₃ (τ) of 19.7° (Figure S3). It has been reported that an increase on the torsion angle minimizes repulsive overlap of the out-of-plane metal $d\pi$ orbitals on adjacent palladium(I) centers [58-61] (which are minimal at 45°). The twist conformation also allows the ligands to span a shorter Pd^I-Pd^I bond [58-61]. In this context, complex **4** exhibits the shortest Pd^I-Pd^I distance [2.3998(8) Å] of the dipalladium(I)-triazenide complexes reported [34,41-43]. Besides, to the best of our knowledge, the related dipalladium(I)-naphthyridine complex (**a**) (Figure 3) reported by Bera and co-

workers [24] is the only other dipalladium(I) complex with a shorter Pd^I-Pd^I distance than **4**, by 0.0046 Å. Thus, for comparison a selected list of N^N-bridging-dipalladium(I) complexes along with their Pd^I-Pd^I distances are collected in Table 1.

Table 1. Comparison of Pd^I-Pd^I bond lengths in selected N^N-bridging-dipalladium(I) complexes.^a

| complex | d _{Pd-Pd} (Å) | Ref. |
|--|------------------------|--------------|
| a [Pd ₂ (μ- <i>acfNP</i>) ₂](BF ₄) ₂ | 2.3952(8) | [24] |
| b [Pd ₂ (μ- <i>NPN</i>) ₂](BF ₄) ₂ | 2.5489(7) | [46] |
| c [Pd ₂ (μ- <i>dpfam</i>)(η ³ -allyl)] | 2.6073(3) | [47] |
| d [Pd ₂ (μ- <i>qaam</i>)(η ³ -allyl)] | 2.5260(2) | [47] |
| e [Pd ₂ (Ar- <i>NNN</i> -Ar') ₂] (Ar = <i>o</i> -CO ₂ Me, Ar' = <i>o</i> -Cl) | 2.4277(5) | [41] |
| f [Pd ₂ (Ar- <i>NNN</i> -Ar') ₂] (Ar = Ar' = <i>o</i> -Cl) | 2.4228(3) | [42] |
| g [Pd ₂ (Ar- <i>NNN</i> -Ar') ₂] (Ar = Ar' = <i>o</i> -Br) | 2.5235(4) | [43] |
| 1 | 2.4309(3) | [34] |
| 2 | 2.4202(3) | [34] |
| 3 | 2.4158(4) | [34] |
| 4 | 2.3998(8) | ^b |

^aAbbreviations: *NPN* = 2,2'-((phenylphosphanediy)bis(methylene))bis(4,5-dihydrooxazole), *dpfam* = *N,N'*-bis[2-(diphenylphosphino)phenyl]formamidinate, *qaam* = *N,N'*-di-8-quinolylacetamidinate, *acfNP* = [(5,7-dimethyl-1,8-naphthyridin-2-yl)amino]carbonylferrocene. ^bThis work.

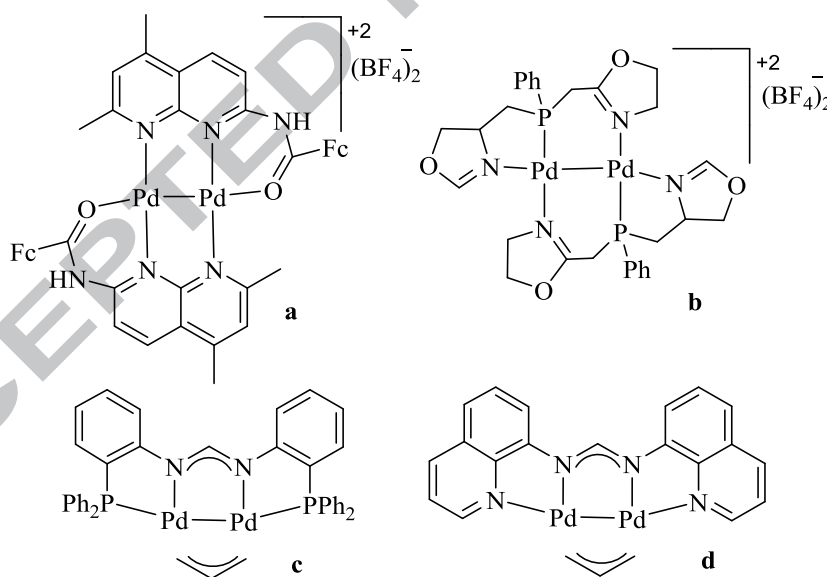


Figure 3. Dipalladium(I) complexes **a-d**.

The short Pd^I-Pd^I distances in these complexes can be related to a constrained ligand bite, weak axial coordination [24,34] and the torsion angle previously discussed. This behavior can be better observed in Figure 4, which shows that for complexes **1** [2.4309(3) Å], **2** [2.4202(3) Å] and **4** [2.3998(8) Å] the Pd^I-Pd^I distance decreases as the torsion angle (τ) increases [**1** (0.4°), **2** (3.2°) and **4** (19.7°)]. However, complex **3** with a Pd^I-Pd^I distance of

2.4158(4) Å and torsion angle (τ) of 0.87°, lays out this trend due to the different *ortho*-substituent coordinated to the Pd^I-Pd^I axis (*o*-methoxy). The influence of the axial coordination on the Pd^I-Pd^I distances, has also been observed in dipalladium(I)-phosphine [61] and dipalladium(I)-amidinate complexes [47].

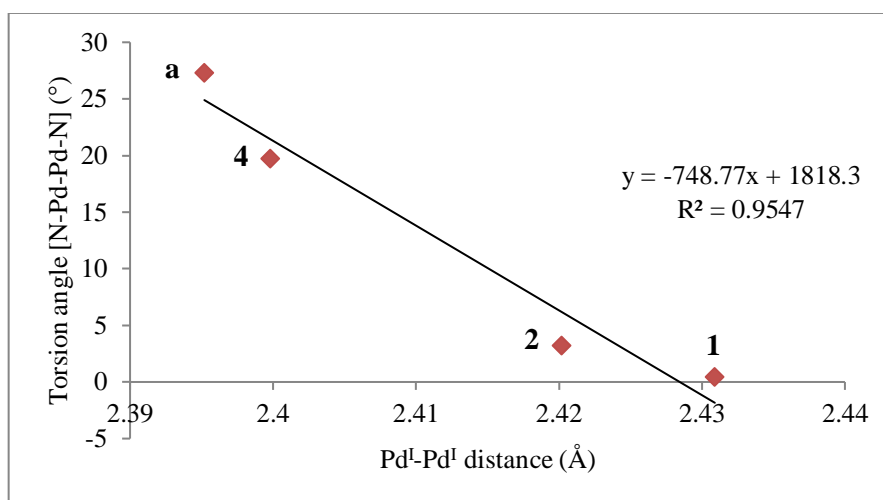


Figure 4. Plot of torsion angles [N₁-Pd-Pd-N₃] (τ) vs Pd^I-Pd^I bond distances for dipalladium(I)-triazenide complexes **1**, **2** and **4**, and the dipalladium(I)-naphthyridine complex **a**.

3.3. Catalysis

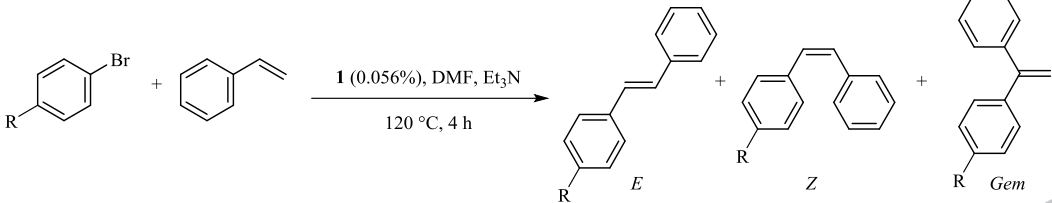
Suzuki [17-23] and Heck couplings [24] as well as other cross-coupling reactions [8-16] mediated by dipalladium(I) complexes have been recently reported. In some cases their catalytic activity has been attributed to the dissociation of the Pd^I-Pd^I complex into Pd^{II} or Pd⁰ catalytic active monomers that start the catalytic cycles [6,16-18]. However, for more robust dipalladium(I) complexes a bimetallic mechanism involving Pd^I-Pd^I/Pd^{II}...Pd^{II} redox cycle has been proposed [10-12,24].

In this context, dipalladium-triazenide complexes **1-6** can be relevant due to the stability beneficial effect of the *ortho*-substituents of the triazenide ligands, which in addition to modulate the oxidation state of the dimetal core [34,38], may confer hemilabile properties to the ligands, whose role would be to provide a coordination site on the metal center and facilitate the binding of the substrates [62-65]. Moreover, the *ortho*-substituted 1,3-bis(aryl)triazenide ligand

as bridging-chelate could suppress the cleavage of the Pd^I-Pd^I core [24,47], allowing a bimetallic mechanism as proposed by Bera and co-workers [24].

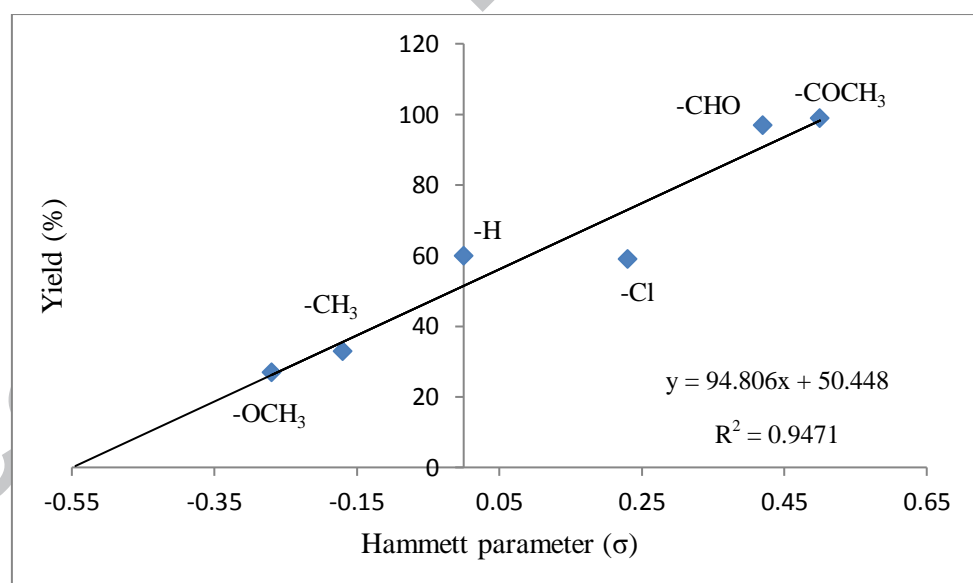
Thus, with the complexes on hand we started the catalytic evaluation of the series of complexes **1-3** in Heck couplings of styrene and bromobenzene, using 0.056% mol of the complexes, DMF as solvent and Na₂CO₃ as base, varying time and reaction temperatures, preparing the samples in the open air. With these experiments (3 h at 150 °C) it was found that complexes **1** and **2** are the best with yields of 67 and 63%, respectively. Noteworthy, raising the reaction temperature above 150 °C, lead to the formation of palladium black. Thus, in order to avoid this, the reaction temperature was reduced to 120 °C. At this temperature, the best catalytic activity was produced by complex **1** (34% at 4 h and 78% at 24 h) albeit reducing the yields and increasing the reaction time. In addition, other organic (DMAP [66,67], NEt₃) and inorganic (Cs₂CO₃) bases were examined, showing NEt₃ to be the best base for the process. In order to further explore the catalytic potential of this complex, Heck couplings were carried out with chlorobenzene, however no conversion was observed with this substrate, probably due to the higher energy required to activate the C-Cl bond [68-70]. Thus, with the best catalyst defined and the reactions conditions optimized a series of Heck couplings with different *para*-substituted bromobenzenes using complex **1** were performed, in order to evaluate the electronic effect of the different substituents of the bromobenzene on the production of stilbenes (Table 2).

The results in Table 2 clearly show, as expected, that bromobenzenes containing the more electron-withdrawing substituents afford the higher yields of the series. These results are in agreement with Hammett parameter values [71]. This behavior can be better observed in Figure 5 where a fairly linear trend is obtained [66,67]. The catalytic activity of complex **1**, in regard to turnover numbers (TON), is better than that obtained by Bera and co-workers with a dipalladium(I)-naphthyridine complex, although they attained higher yields in shorter reaction times [24].

Table 2. Heck couplings of *para*-substituted bromobenzenes with styrene catalyzed by **1**.^a


| Entry | R | Hammett parameter | TON | Yield (%) ^b | E/Z/Gem |
|-------|--------------------|-------------------|------|------------------------|---------|
| 1 | -OCH ₃ | -0.27 | 480 | 27 | 89/11/0 |
| 2 | -CH ₃ | -0.17 | 587 | 33 | 90/10/0 |
| 3 | -H | 0 | 1066 | 60 | 92/8/0 |
| 4 | -Cl | 0.23 | 1049 | 59 | 92/8/0 |
| 5 | -CHO | 0.42 | 1725 | 97 | 97/3/0 |
| 6 | -COCH ₃ | 0.5 | 1760 | 99 | 96/4/0 |

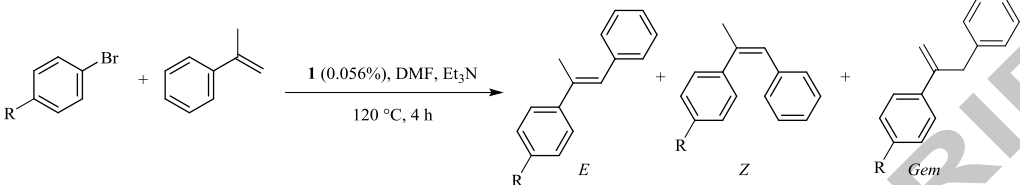
^aConditions: 6.369 mmol of bromobenzene, 6.369 mmol of styrene, 7.640 mmol of Et₃N, 3.582×10^{-3} mmol of complex **1** and 3 mL of DMF. ^bYields obtained by GC are based on remaining bromobenzene and are the average of two runs.

**Figure 5.** Graphic of Hammett parameter (σ) of the *para*-substituted bromobenzenes vs yield of stilbenes.

Similar experiments using *para*-substituted bromobenzenes with α -methyl styrene, under the same reaction conditions using **1** as catalysts, were also successful to produce trisubstituted olefins, however the yields were lower (52-16%) (Table 3), probably due to the

steric effect of the α -methylstyrene [66]. The results attained exhibit a similar trend to that observed for styrene where a linear behavior can be clearly noted (Figure 6).

Table 3. Heck reactions of *para*-substituted bromobenzenes with α -methylstyrene catalyzed by **1**.^a



| Entry | R | Hammett parameter | TON | Yield (%) ^b | E/Z/Gem |
|-------|--------------------|-------------------|-----|------------------------|---------|
| 1 | -OCH ₃ | -0.27 | 284 | 16 | 89/11/0 |
| 2 | -CH ₃ | -0.17 | 302 | 17 | 90/10/0 |
| 3 | -H | 0 | 569 | 32 | 92/8/0 |
| 4 | -Cl | 0.23 | 764 | 43 | 92/8/0 |
| 5 | -CHO | 0.42 | 818 | 46 | 97/3/0 |
| 6 | -COCH ₃ | 0.5 | 523 | 52 | 96/4/0 |

^aConditions: 6.369 mmol of bromobenzene, 6.369 mmol of styrene, 7.640 mmol of Et₃N, 3.582×10^{-3} mmol of catalyst **1** and 3 mL of DMF. ^bYields obtained by GC are based on remaining bromobenzene and are the average of two runs.

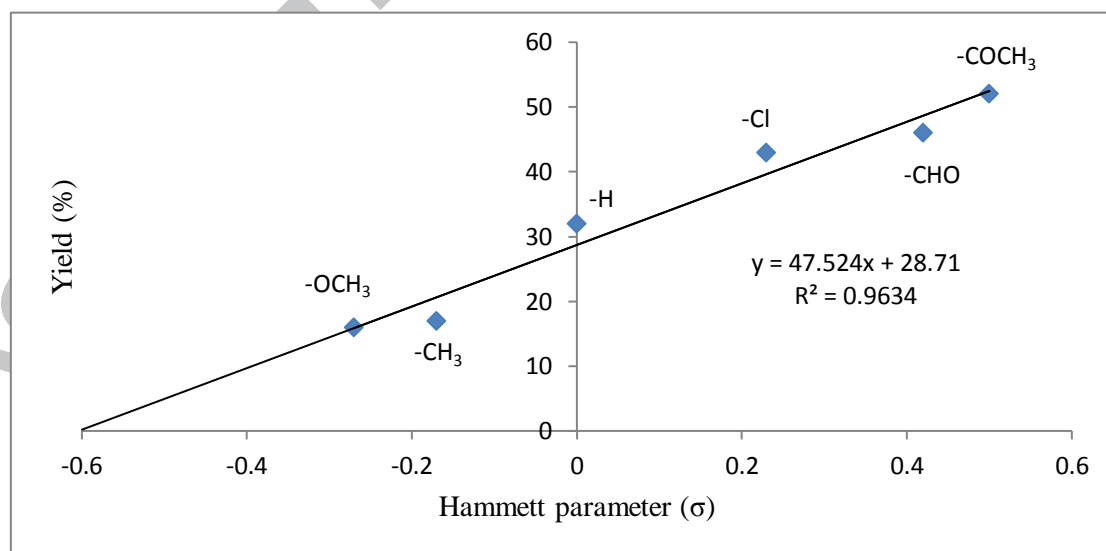
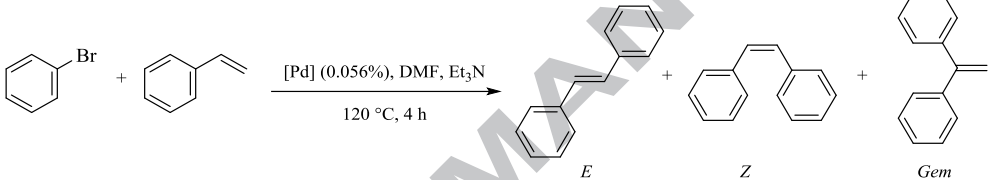


Figure 6. Graphic of Hammett parameter (σ) of the *para*-substituted bromobenzenes vs yield of olefins.

Further, it was important to explore whether the series of complexes **4-6** may exhibit a better performance than compound **1** in similar Heck couplings, as a function of the different *para*-halogen substituents in the 1,3-bis(aryl)triazenide ligands of the complexes, under the same reaction conditions (DMF, NEt₃, 120 °C, 4 h). The results (Table 4) show yields comparable (**4**, 59%; **5**, 60% and **6**, 63%) to those obtained with **1** (60%). Thus, indicating that the electronic effect of the *para*-halogen substituents plays no significant role in the catalytic activities of this series of complexes. However, the presence of a less electronegative *para*-halogen substituent in the 1,3-bis(aryl)triazenide ligand slightly enhances the activity of the catalyst.

Table 4. Catalytic activity of complexes **1**, and **4-6** in Heck couplings.^a



| Entry | Compound | TON | Yield (%) ^b | <i>E/Z/Gem</i> |
|-------|----------|------|------------------------|----------------|
| 1 | 1 | 1066 | 60 | 92/8/0 |
| 2 | 4 | 1049 | 59 | 92/7/1 |
| 3 | 5 | 1066 | 60 | 89/10/1 |
| 4 | 6 | 1120 | 63 | 90/10/0 |

^aConditions: 6.369 mmol of bromobenzene, 6.369 mmol of styrene, 7.640 mmol of Et₃N, 3.582×10^{-3} mmol of catalyst (**1**, **4-6**) and 3 mL of DMF. ^bYields obtained by GC are based on remaining bromobenzene and are the average of two runs.

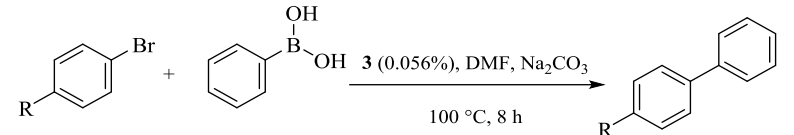
Suzuki couplings

With the good results obtained in the Heck couplings it was decided to expand the catalytic scope of the series of complexes **1-3** in Suzuki-Miyaura couplings of bromobenzene and phenylboronic acid for the production of biphenyl. Initially, reactions were performed using the optimized conditions found for the Heck couplings (0.056% mol catalyst, DMF and Na₂CO₃) while the reaction time and temperatures were varied. The results showed complex **3** to be the best catalyst at different reaction temperatures (80, 100 and 120 °C), from which 100 °C, was chosen as the optimal, attaining 63% yield of biphenyl after 6 h of reaction. Noteworthy

the fact that in the Heck couplings, complex **1** was the best catalysts and complex **3** was one of the less active. This may lead to infer that is in fact the nature of the functional groups at the *ortho*-position of the 1,3-bis(aryl)triazene ligands affecting and thus it can be modulated in order to improve the catalytic properties of their complexes [38-40].

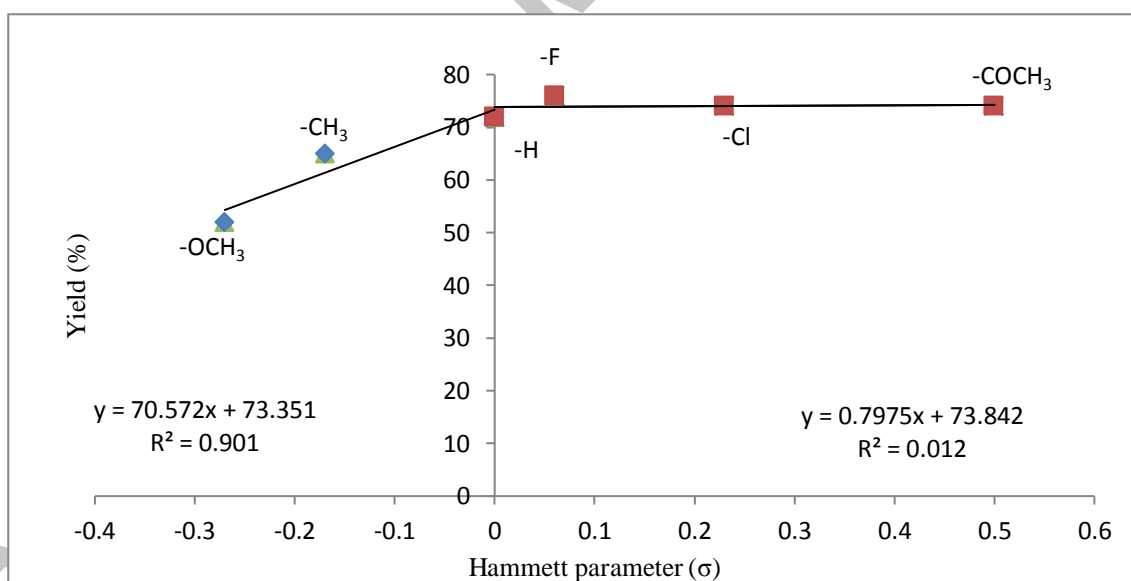
Further, given the fundamental importance that the base plays in Suzuki-Miyaura couplings, other alkaline carbonates were used at 100 °C, 8 h (reaction time was increased from 6 to 8 h to have better yields with bases such as Li_2CO_3 that exhibited very low yields at the above chose reaction time of 6 h) of reaction and complex **3** as catalyst (0.056% mol). The best yields were obtained using Na_2CO_3 (71 %) and Cs_2CO_3 (73%), while other bases employed afforded reduced conversions (Li_2CO_3 41%; K_2CO_3 63%; Rb_2CO_3 67%). Based on the slight yield differences observed for Cs_2CO_3 and Na_2CO_3 and on the prices of these chemicals we decided to continue our studies using Na_2CO_3 as the selected base.

Thus, under these optimized conditions (0.056% mol of catalyst, Na_2CO_3 , DMF, 100 °C, 8 h) the catalytic activity of complex **3** towards a series of *para*-substituted bromobenzenes was explored [72-76] (Table 5). Once again, as expected, the results showed that bromobenzenes having electron-withdrawing *para*-substituents were more active than those with electron-donating groups. The conversion increases as a direct function of the Hammett parameter [71] of the *para*-substituents, reaching the highest conversion of 76% for the *p*-F bromobenzene. However, by increasing the Hammett parameter to 0.23 (*p*-Cl-bromobenzene) and 0.5 (*p*- COCH_3 -bromobenzene) a slightly decrease in conversion was observed (74%) (Figure 7). As suggested by Scheck [77] and Norrby [78], a concave-downwards Hammett plot, may suggest a change in the rate-determining step resulting from the different electronic contributions of the substituents.

Table 5. Suzuki couplings of *para*-substituted bromobenzenes with phenylboronic acid catalyzed by **3**.^a


| Entry | R | Hammett parameter | TON | Yield (%) ^b |
|-------|--------------------|-------------------|------|------------------------|
| 1 | -OCH ₃ | -0.27 | 925 | 52 |
| 2 | -CH ₃ | -0.17 | 1156 | 65 |
| 3 | -H | 0 | 1280 | 72 |
| 4 | -F | 0.06 | 1351 | 76 |
| 5 | -Cl | 0.23 | 1316 | 74 |
| 6 | -COCH ₃ | 0.5 | 1316 | 74 |

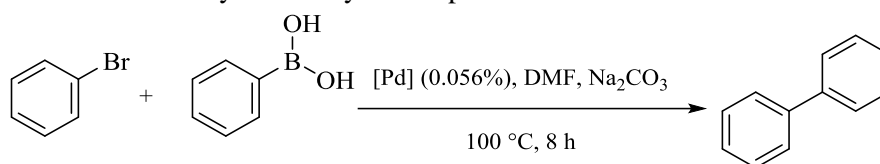
^aConditions: 6.369 mmol of bromobenzene, 6.369 mmol of phenylboronic acid, 7.640 mmol of Na₂CO₃, 3.582 × 10⁻³ mmol of catalyst **3** and 3 mL of DMF. ^bYields obtained by GC are based on remaining bromobenzene and are the average of two runs.

**Figure 7.** Graphic of Hammett parameter of the *para*-substituent in bromobenzene vs yield of biphenyl.

Complexes **4-6** were also used as catalysts for Suzuki couplings under optimized conditions (Table 6). Complex **4** with the more electronegative *para*-halogen substituent (*p*-F) shows the best activity with a yield of 76%, whereas, **5** (*p*-Cl) and **6** (*p*-Br) show yields of 75 and 73%, respectively. This trend contrasts with the results obtained in the Heck reaction (Table

4) where the presence of a less electronegative *para*-halogen substituent enhances slightly the activity of the catalyst.

Table 6. Catalytic activity of complexes **4-6** in the Suzuki reaction.^a



| Entry | complexes | TON | Yield (%) ^b |
|-------|-----------|------|------------------------|
| 1 | 4 | 1351 | 76 |
| 2 | 5 | 1333 | 75 |
| 3 | 6 | 1298 | 73 |

^aConditions: 6.369 mmol of bromobenzene, 6.369 mmol of phenylboronic acid, 7.640 mmol of Na₂CO₃, 3.582 × 10⁻³ mmol of catalyst (**4-6**) and 3 mL of DMF. ^bYields obtained by GC are based on remaining bromobenzene and are the average of two runs.

4. Conclusions

A series of dipalladium(I)-triazenide complexes [Pd{1-(2'-methoxycarbonylphenyl)-3-(4'-X-phenyl)triazenide}]₂ [X = F (**4**); Cl (**5**); Br (**6**)] have been synthesized and fully characterized by IR, NMR and HRMS. The crystal structure of **4** determined by X-ray diffraction studies show some common features with other dipalladium(I)-triazenide complexes, but also some significant differences, since the eight-membered Pd₂(NNN)₂ ring adopts a "twist boat configuration" with the higher torsion angle [N₁-Pd₁-Pd₁-N₃ (τ), 19.7°] and the shortest Pd^I-Pd^I distance [2.3998(8) Å] among dipalladium(I)-triazenide complexes. Pd(I) complexes have the advantage of being used as catalysts under air. Therefore, the series of dipalladium(I)-triazenide complexes **1-3** were tested as catalysts in Heck and Suzuki-Miyaura couplings. Under optimized conditions, complex **1** exhibited the highest activity in the Heck reaction, while complex **3** showed to be the best in the Suzuki coupling, suggesting their efficiencies to be dependent on the *ortho*-substituent in the triazenide ligand. Complex **1** is also an efficient catalyst for the olefinic coupling of different *para*-substituted bromobenzenes with both styrene and *α*-methylstyrene, producing better yields with bromobenzenes containing electron-

withdrawing substituents. Complex **3** was efficient in the coupling of phenylboronic acid with a series of *para*-bromobenzenes. Additionally, complexes **4-6** were tested as catalysts, showing comparable yields with complex **1** in the Heck reaction, and comparable yields with compound **3** in the Suzuki reaction, indicating the *para*-halogen substituent in the triazenide ligands to play no significant role in the catalytic activity of these complexes.

Acknowledgements

This work was supported by Consejo Nacional de Ciencia y Tecnología (CONACyT) Grant 60467 and Dirección General de Educación Tecnológica (DGEST) Grant 5150.13-P. E.C.-A (349527) and C.C.-A (183618) thank CONACyT for graduate fellowships. We thank CONACyT for ITT NMR and HRMS facilities (Grants INFR-2011-3-173395 and INFR-2012-01-187686). E.C.-A. thanks Dr. A. Zajac of ESET, LLC for complementary financial support.

Supplementary material

CCDC 1859275 (**4**), contains the supplementary crystallographic data for this paper. These data can be obtained free of charge from The Cambridge Crystallographic Data Centre via www.ccdc.cam.ac.uk/data_request/cif.

Supplementary data associated with this article can be found, in the online version, at <http://xxxxxxxxxxx>

References

1. I.G. Powers, C. Uyeda, *ACS Catal.* 7 (2017) 936-958.
2. D.R. Pye, N.P. Mankad, *Chem. Sci.* 8 (2017) 1705-1718.
3. D.C. Powers, T. Ritter, *Accounts of Chemical Research* 45 (2012) 840-850.
4. N.P. Mankad, *Chem. Commun.* 54 (2018) 1291-1302.
5. C.-S. Cao, Y. Shi, H. Xu, B. Zhao, *Coord. Chem. Rev.* 365 (2018) 122-144.
6. T. Inatomi, Y. Koga, K. Matsubara, *Molecules* 23 (2018) 140-161.
7. K.O. Kirlikovali, E. Cho, T.J. Downard, L. Grigoryan, Z. Han, S. Hong, D. Jung, J.C. Quintana, V. Reynoso, S. Ro, Y. Shen, K. Swartz, E.T. Sahakyan, A.I. Wixtrom, B. Yoshida, A.L. Rheingold, A.M. Spokoyny, *Dalton Trans.*, 47 (2018) 3684-3688.
8. I. Kalvet, G. Magnin, F. Schoenebeck, *Angew. Chem. Int. Ed.* 56 (2017) 1581-1585.
9. I. Kalvet, T. Sperger, T. Scattolin, G. Magnin, F. Schoenebeck, *Angew. Chem. Int. Ed.* 56 (2017) 7078-7082.
10. G. Yin, I. Kalvet, F. Schoenebeck, *Angew. Chem.* 127 (2015) 6913-6917.
11. M. Aufiero, T. Sperger, A. S. K. Tsang, F. Schoenebeck, *Angew. Chem., Int. Ed.*, 54 (2015) 10322-10326.
12. G. Yin, I. Kalvet and F. Schoenebeck, *Angew. Chem., Int. Ed.*, 54 (2015) 6809-6813.
13. I. Kalvet, K.J. Bonney, F. Schoenebeck, *J. Org. Chem.* 79 (2014) 12041-12046.
14. J.P. Stambuli, R. Kuwano, J.F. Hartwig, *Angew. Chem. Int. Ed.* 41 (2002) 4746-4748.
15. U. Christmann, D.A. Pantazis, J. Benet-Buchholz, J.E. McGrady, F. Maseras, R. Vilar, J. Am. Chem. Soc. 128 (2006) 6376-6390.
16. C.C.C. Johansson-Seechurn, T. Sperger, T.G. Scrase, F. Schoenebeck, T.J. Colacot *J. Am. Chem. Soc.* 139 (2017) 5194-5200.
17. T.E. Barder, *J. Am. Chem. Soc.* 128 (2006) 898-904.
18. D.P. Hruszkewycz, D. Balcells, L.M. Guard, N. Hazari, M. Tilset, *J. Am. Chem. Soc.* 136 (2014) 7300-7316.
19. F. Proutiere, M. Aufiero, F. Schoenebeck, *J. Am. Chem. Soc.* 134 (2012) 606-612.
20. X. Han, Z. Weng, T.S.A. Hor, *J. Organomet. Chem.* 692 (2007) 5690-5696.

21. F. Proutiere, E. Lyngvi, M. Aufiero, I.A. Sanhueza, F. Schoenebeck, *Organometallics* 33 (2014) 6879-6884.
22. D.P. Hruszkewycz, L.M. Guard, D. Balcells, N. Feldman, N. Hazari, M. Tilstet, *Organometallics* 34 (2015) 381-394.
23. M. Aufiero, T. Scattolin, F. Proutiere, F. Schoenebeck, *Organometallics* 34 (2015) 5191-5195.
24. R.J. Das, B. Saha, S.M.W. Rahaman, J.K. Bera, *Chem. Eur. J.* 16 (2010) 14459-14468.
25. E. Hartmann, J. Strähle, *Z. Naturforsch.* 43b (1988) 818-824.
26. C.-D. Leger, G. Maas, *Z. Naturforsch.* 59b (2004) 573-578.
27. N.G. Connelly, O.D. Hayward, P. Klanginsirikul, A.G. Orpen, *J. Chem. Soc. Dalton Trans.* (2002) 305-306.
28. C.J. Adams, R.A. Baber, N.G. Connelly, P. Harding, O.P. Hayward, M. Kandiah, A.G. Orpen, *Dalton Trans.*, (2006) 1749-1757.
29. W.-T. Lee, M. Zeller, A. Lugosan, *Inorg. Chim. Acta* 477 (2018) 109-113.
30. A. Singhal, V.K. Jain, M. Nethaji, A.G. Samuelson, D. Jayaprakash, R.J. Butcher, *Polyhedron* 17 (1998) 3531-3540.
31. J. Ruiz, J.F.J. López, V. Rodríguez, J. Pérez, M.C. Ramírez de Arellano, G. López, J. *Chem. Soc. Dalton Trans.*, (2001) 2683-2689.
32. G. García-Herbosa, N.G. Connelly, A. Muñoz, J.V. Cuevas, A.G. Orpen, S.D. Politzer, *Organometallics* 20 (2001) 3223-3229.
33. J. Chu, Q.-y. Lv, J.-p. Cao, X.-h. Xie, S. Zhan, *Inorg. Chem. Commun.* 36 (2013) 245-248.
34. J.J. Nuricumbo-Escobar, C. Campos-Alvarado, G. Ríos-Moreno, D. Morales-Morales, P.J. Walsh, M. Parra-Hake, *Inorg. Chem.* 46 (2007) 6182-6189.
35. J.G. Rodríguez, M. Parra-Hake, G. Aguirre, F. Ortega, P.J. Walsh, *Polyhedron* 18 (1999) 3051-3055.
36. G. Ríos-Moreno, G. Aguirre, M. Parra-Hake, P.J. Walsh, *Polyhedron* 22 (2003) 563-568.
37. C. Tejel, M.A. Ciriano, G. Ríos-Moreno, I.T. Dobrinovitch, F.J. LaHoz, L.A. Oro, M. Parra-Hake, *Inorg. Chem.* 43 (2004) 4719-4726.

38. J.J. Nuricumbo-Escobar, C. Campos-Alvarado, F. Rocha-Alonso, G. Ríos-Moreno, D. Morales-Morales, H. Höpfl, M. Parra-Hake, *Inorg. Chim. Acta* 363 (2010) 1150-1156.
39. E. Correa-Ayala, A. Valle-Delgado, G. Ríos-Moreno, D. Chávez, D. Morales-Morales, S. Hernández-Ortega, J.J. García, M. Flores-Álamo, V. Miranda-Soto, M. Parra-Hake, *Inorg. Chim. Acta* 446 (2016) 161-168.
40. E. Correa-Ayala, C. Campos-Alvarado, D. Chávez, D. Morales-Morales, S. Hernández-Ortega, J.J. García, M. Flores-Álamo, V. Miranda-Soto, M. Parra-Hake, *Inorg. Chim. Acta* 466 (2017) 510-519.
41. J. Chu, Q-y. Lv, X-h. Xie, W. Li, S. Zhan, *Transition Met. Chem.* 38 (2013) 843-847.
42. J. Chu, X-h. Xie, S-r. Yang, S. Zhan, *Inorg. Chim. Acta* 410 (2014) 191-194.
43. S. Ibañez, L. Oresmaa, F. Estevan, P. Hirva, M. Sanaú, M.A. Úbeda, *Organometallics* 33 (2014) 5378-5391.
44. M.S. Kharasch, R.C. Seyler, R.F. Mayo, *J. Am. Chem. Soc.* 60 (1938) 882-884.
45. G.M. Sheldrick. *Acta Cryst.* (2015). C71, 3-8.
46. J. Zhang, R. Pattacini, P. Braunstein, *Inorg. Chem.* 48 (2009) 11954-11962.
47. Y. Yamaguchi, K. Yamanishi, M. Kondo, N. Tsukada, *Organometallics* 32 (2013) 4837-4842.
48. S. Lin, D.E. Herbert, A. Velian, M.W. Day, T. Agapie, *J. Am. Chem. Soc.* 135 (2013) 15830-15840.
49. M. Wada, N. Takahashi, Y. Inoue, N. Tsukada, *J. Organomet. Chem.* 694 (2009) 1333-1338.
50. S.K. Bhargava, S.H. Privér, A.C. Willis, M.A. Bennett, *Organometallics* 31 (2012) 5561-5572.
51. D.P. Hruszkewycz, J. Wu, C.D. Incarvito, N. Hazari, *J. Am. Chem. Soc.* 133 (2011) 3280-3283.
52. S. Oldenhof, M. Lutz, B. de Bruin, J.I. van der Vlugt, J.N.H. Reek, *Organometallics* 33 (2014) 7293-7298.

53. C.M. Fafard, D. Adhikari, B.M. Foxman, D.J. Mindiola, O.V. Ozerov, *J. Am. Chem. Soc.* 129 (2007) 10318-10319.
54. J.R. Walensky, C.M. S.F. Colson, S.D. Robinson, *Polyhedron* 7 (1988) 1919-1924.
55. C.L. Lu, J.C. Peters, *J. Am. Chem. Soc.* 126 (2004) 15818-15832.
56. M.P. Rančić, N.P. Trišović, M.K. Milčić, I.A. Ajaj, A.D. Marinković, *J. Mol. Struct.* 1049 (2013) 59-68.
57. D.M. Khramov, C.W. Bielawski *J. Org. Chem.* 72 (2007) 9407-9417.
58. M.K. Kullberg, F.R. Lemke, D.R. Powell, C.P. Kubiak, *Inorg. Chem.* 24 (1985) 3589-3593.
59. T.E. Krafft, C.I. Hejna, J.S. Smith, *Inorg. Chem.* 29 (1990) 2682-2688.
60. M. Tanaka, K. Tani, K. Mashima, *Inorg. Chem.* 35 (1996) 5244-5248.
61. G. Bensenyei, L. Párkányi, E. Gács-Baitz, B.R. James, *Inorg. Chim. Acta* 327 (2002) 179-187.
62. A. Bader, E. Lindner, *Coord. Chem. Rev.* 108 (1991) 27-110.
63. P. Braunstein, F. Naud, *Angew. Chem., Int. Ed.* 40 (2001) 680-699.
64. Y.-C. Lin, H.-H. Hsueh, S. Kanne, L.-K. Chang, I.J.B. Lin, G.-H. Lee, S.-M. Peng, F.-C. Liu, *Organometallics*, 32 (2013) 3859-3869.
65. R. Lindner, B. van der Bosch, M. Lutz, J.N.H. Reek, J.I. van der Vlugt, *Organometallics* 30 (2011) 499-510.
66. F.E. Hahn, M.C. Jahnke, V. Gomez-Benitez, D. Morales-Morales, T. Pape, *Organometallics* 24 (2005) 6458-6463.
67. A. Naghipour, S.J. Sabounchei, D. Morales-Morales, D. Cansero-González, C.M. Jensen, *Polyhedron* 26 (2007) 1445-1448.
68. R.B. Bedford, C.S.J. Cazin, D. Holder, *Coord. Chem. Rev.* 248 (2004) 2283-2321.
69. J. Ye, X. Zhang, W. Chen, S. Shimada, *Organometallics* 27 (2008) 4166-4172.
70. S.K. Yen, L.L. Koh, F.F. Hahn, H.V. Huynh, T.S.A. Hor, *Organometallics* 25 (2006) 5105-5112.
71. C. Hansch, A. Leo, R.W. Taft, *Chem. Rev.* 91(1991) 165-195.

72. M. Basauri-Molina, S. Hernández-Ortega, R.A. Toscano, J. Valdés-Martínez, D. Morales-Morales, *Inorg. Chim. Acta* 363 (2010) 1222-1229.
73. P. Conelly-Espinosa, D. Morales-Morales, *Inorg. Chim. Acta* 363 (2010) 1311-1315.
74. F. Estudiante-Negrete, S. Hernández-Ortega, D. Morales-Morales, *Inorg. Chim. Acta* 387 (2012) 58-63.
75. C. Crisóstomo-Lucas, R.A. Toscano, D. Morales-Morales, *Tetrahedron Letters* 54 (2013) 3116-3119.
76. S. Ramírez-Rave, F. Estudiante-Negrete, R.A. Toscano, S. Hernández-Ortega, D. Morales-Morales, J.-M. Grévy, *J. Organomet. Chem.* 749 (2014) 287-295.
77. J.O. Scheck, *J. Chem. Educ.* 48 (1971) 103-107.
78. P. Fristrup, S.L. Quement, D. Tanner, P.-O. Norrby, *Organometallics* 23 (2004) 6160-6165.